Title

Endowment of pH responsivity to anticancer peptides by introducing 2,3-diaminopropionic acid residues

Authors

Naoto Tanishiki, Yoshiaki Yano, Katsumi Matsuzaki*

Graduate School of Pharmaceutical Sciences, Kyoto University, Kyoto 606-8501 (Japan)

E-mail: mkatsumi@pharm.kyoto-u.ac.jp

Abstract

Endowment of pH responsivity to anticancer peptides is a promising approach to achieve better selectivity to cancer tissues. In this research, a template peptide was designed based on magainin 2, an antimicrobial peptide with anticancer activity, and a series of peptides were designed by replacing different numbers of lysine with the unnatural amino acid, 2,3-diaminopropionic acid (Dap), which has a positive charge at weakly acidic pH in cancer tissues, but is neutral at physiological pH 7.4. These Dap-containing peptides are expected to interact more strongly with tumor cells than with normal cells because 1) a weakly acidic condition is formed in tumors, and 2) the membrane of tumor cells is more anionic than that of normal cells. While all examined peptides showed potent cytotoxicities to multidrug-resistant cancer cells at a weakly acidic pH (ED_{50} ~5 μM), the toxicity was decreased with an increase in the number of Dap at pH 7.4 (8 Dap residues resulted in ED_{50} ~60 μM). Furthermore, the

introduction of Dap reduced cytotoxicity against normal cells. Thus, Dap introduction significantly improved cancer targeting due to a pH-dependent charge shift. Fluorescence imaging and model membrane experiments supported this charge shift model.

Introduction

Cancer is one of the most common fatal disease around the world. It ranked as the first or second cause of death in people under 70 of age in over 90 countries in 2015.[1] Despite considerable efforts, there are many barriers to overcome the disease with chemotherapy, in particular side effects[2] and drug resistance.[3, 4] Therefore, drugs with new modes of action are urgently needed.

Natural antimicrobial peptides play an important role in the innate immunity of plants and animals, including humans.[5] These peptides typically have many basic residues and cationic amphipathic structures suitable for interaction with the anionic cell membranes of microorganisms. Several antimicrobial peptides also have anticancer activity.[6] Cells acquire little resistance to anticancer peptides because they exert cytotoxicity by permeabilizing lipid bilayers without interacting with specific receptors.[7] Because of their activities toward multidrug-resistant cancer cells, anticancer peptides have been researched as promising candidates for cancer treatment. While cationic anticancer peptides target cancer cells based on the anionic charges of cancer cell cellular membranes,[8-10] their insufficient cell selectivities to cancer cells remain problematic, and they are also toxic to normal cells.[9]

A promising approach for better tissue selectivity is endowment of pH responsivity to

anticancer peptides. The pH value in tumor tissue (5.6 - 6.8[11] or 6.2 - 6.9[12]) is lower than that in normal tissue (~ 7.4). This is achieved primarily due to activation of the Na^+/H^+ exchanger and the H^+/lactate cotransporter [12]. The proton secretion ability increases with tumor aggressiveness[12]. Metastatic or multidrug-resistant cancer tissues are considered to have even lower pH than other cancer tissues.[11, 13] In our previous research, the acidic environment in cancer tissues was used to improve the selectivity of F5W-substituted magainin 2 (MG),[14] a well-studied anticancer peptide isolated from *Xenopus laevis*.[15] A peptide with larger cationic charges at a weakly acidic pH than at neutral pH should exhibit stronger electrostatic interaction with anionic membranes in cancer tissues. Such acidity responsive tumoricidal (ART) peptides are expected to exert more potent effects against progressed cancers. We previously designed an ART peptide by introducing 6 His residues (pK_a ~ 6.0) into an MG analog,[14] but the anticancer activity was not sufficient.

In this research, we introduced 2,3-diamino propionic acid (Dap, Figure1a) residues into a MG-based template peptide to improve pH responsivity. Dap is a non-proteinogenic amino acid found in several species of plants,[16] biosynthesis of antibiotics[17] and meteorites.[18] The pK_a value of the Dap side chain in a peptide is ~ 6.3,[19] so it is more sensitive to acidification in cancer tissues than His. The template peptide was designed by introducing Lys residues into MG, and a series of peptides were generated by replacing several lysine residues with Dap.

While all peptides exhibited potent cytotoxicities to a human pancreas carcinoma cell line PANC-1 at pH 6.0 (ED_{50} ~ 5 μM), the toxicity was decreased with an increase in the number of Dap

residues at pH 7.4 (ED_{50} ~ 60 μM for a peptide with 8 Dap residues). Furthermore, the introduction of Dap also reduced cytotoxicity against normal human embryonic kidney cells 293 (HEK293) and glomerular mesangial (GM) cells at pH 7.4 (ED_{50} > 100 μM).

Results

Peptide design

The template peptide 0Dap was designed based on MG. Four Lys residues were introduced into the hydrophilic face of helix of MG instead of Gly^{3}, Ala^{15}, Gly^{18}, and Glu^{19} and the C-terminal carboxyl group was amidated to increase the net positive charge (Table 1, Figure S1 for the helical wheel diagram). Additionally, Met^{21} was replaced with norleucine (Nle, Figure 1b) to avoid Met oxidization. Dap-containing peptides were designed by replacing cationic Lys residues (pK_a ~ 10) of 0Dap with pH-responsive Dap residues (pK_a~ 6.3) named based on their Dap numbers (Table 1). 0Dap is expected to have + 8.5 and + 9.5 positive charges at physiological pH 7.4 and acidic pH 6.0, respectively, due to amino groups of eight Lys side chains, the N-terminus, and the side chain of His. Dap residue has a lower pKa value than Lys. Dap-containing peptides are expected to have larger responsive charge shifts (Table 1).

pH-dependent cytotoxicity

Multidrug-resistant PANC-1 cells derived from a human pancreatic ductal carcinoma were utilized to

evaluate the anticancer activity of the peptides.[3] The cells were confirmed to be resistant to mitomycin C, a typical anticancer drug, both at pH 6.0 and 7.4 (Figure 2).

The cytotoxicity of each peptide was examined at different extracellular pH conditions between 6.0 and 7.4 (Figure 3). The EC_{50} value was calculated by fitting the data to the equation

$$V = \frac{100}{1+(\frac{C}{EC50})^a} \quad (1)$$

(V, C and a represent cellular viability, peptide concentration and cooperativity index, respectively) for each condition (Figure 3). Each peptide exhibited comparable potent toxicity at pH 6.0 (EC_{50} of ~5 μM), while the toxicity was decreased with an increase in the number of Dap residues at pH 7.4 (EC_{50} of ~9 μM and ~ 60 μM for 0Dap and 8Dap, respectively). Thus, Dap introduction endowed ART activity toward the peptide.

The toxicity of each peptide against normal GM and HEK293 cells was determined compared with that against cancer PANC-1 cells (Figure 4, Table 2). The kidney-derived GM cells were examined both at weakly acidic pH 6.0 and physiological pH 7.4 because the normal kidney has acidic regions in certain cases.[20] While all peptides exhibited PANC-1 selectivity at both pH 6.0 and 7.4, it increased with the number of Dap residues. These results suggested enhanced selectivity of Dap-containing peptides to cancer cells due to their sensitivity to low pH in addition to stronger electrostatic interactions to the more anionic cancer plasma membranes.

Localization of peptides in PANC-1 cells

To investigate the peptide cytotoxicity mechanisms, Alexa488 conjugated 0Dap and 8Dap were synthesized. The cytotoxicities of these labeled peptides against PANC-1 cells were comparable to those of the free-peptides (Figure S2). Therefore, we assume that the labeled peptides have similar action mechanisms in the cells as the corresponding unlabeled peptides.

PANC-1 cells were incubated with 0.2 μM of the labeled peptides for 24 h in pH-adjusted medium to evaluate the peptide uptake from the fluorescence intensity of each cell (Figure 5). At pH 6.0, both peptides exhibited similar uptake, whereas at pH 7.4, 8Dap exhibited weaker uptake, in good agreement with the cytotoxicity (Figure 3). At pH 6.0, 0Dap exhibited a slightly weaker signal than at pH 7.4, possibly because the ATP-dependent active uptake by cells was weakened at pH 6.0.

PANC-1 cells were also treated with 0.2 μM of the labeled peptides with EC_{50} concentrations of the unlabeled peptides. Mitochondria were stained with Mito Tracker, a membrane potential-dependent mitochondrial dye (Figure 6). Cells were time-lapse imaged at pH 6.0 or 7.4 for 30 minutes, and rapid internalization was observed under the conditions in which potent cytotoxicities were observed (0Dap at both pH values and 8Dap at pH 6.0). The internalization of the peptides was completed in a few minutes and the fluorescence of Mito Tracker vanished simultaneously, indicating loss of the mitochondrial membrane potential.

Liposome interaction

To elucidate the mechanisms of the pH dependence, the interactions between liposomes and peptides were examined. The affinity of the peptides to lipid bilayers was evaluated based on the blue-shift of Trp fluorescence, which is known to indicate less polar environments in membranes. 1-palmitoyl-2-oleoyl-*sn*-glycero-3-phosphocholine (POPC) and 1-palmitoyl-2-oleoyl-*sn*-glycero-3-phosphoserine (POPS) were used as zwitterionic and anionic phospholipids. Two lipid compositions of large unilamellar vesicles (LUVs) (POPC: POPS: cholesterol = 8: 1: 1 or 9: 0: 1) were prepared to measure the membrane binding of 0Dap or 8Dap (Figure 7). The requirement of negatively charged lipids (POPS) for binding of the peptides indicates the importance of electrostatic interactions, as mentioned in the literature.[21] While both peptides exhibited similar binding affinities at pH 6.0 (Figure 7a), 8Dap was less likely to bind to anionic lipid membranes than 0Dap at pH 7.4 (Figure 7b).

The secondary structures of the peptides in the absence and presence of vesicles were estimated by CD (Figure 8 and Table 3). At pH 6.0, both peptides with LUVs (*L/P* = 100) exhibited double-minima at 208 and 222 nm, indicating helical structures; however, 8Dap was significantly less structured (Figure 8a). On the other hand, at pH 7.4, both peptides assumed similar helical structures in the presence of LUVs (Figure 8b). Fluoride did not significantly affect the peptide–membrane interaction because in NaCl buffer, similar $[\theta]_{222}$ value of ~22,000 deg cm^2 dmol^{-1} was observed for 0Dap at pH7.4 in the presence of the LUVs., although CD spectra below 200 nm could not be measured

in NaCl buffer.

Peptide-induced leakage of calcein encapsulated in LUVs was determined to evaluate the membrane-permeabilizing activities of the two peptides (Figure 9). The leakage was not dependent on pH. At both pH values, 0Dap exhibited stronger membrane-permeabilizing activities than 8Dap.

Discussion

Cellular selectivity

As shown in previous studies, cationic anticancer peptides possess cancer selectivity[6, 9, 10] because they have more cancer cell anionic plasma membranes than those of normal cells due to larger surface expressions of phosphatidylserine, sialic acid and glycosaminoglycans.[9] Consistently, all peptides examined in this study were cancer cell-selective. In addition to the difference in surface charge of membranes, ART peptides are assumed to have another mechanism of cell selectivity. The pH values just above the lipid membranes decreased as the anionic components of the membranes increased.[14, 22] ART peptides become more cationic just above cancer cell membranes than above normal cell membranes. Therefore, ART peptides have the potential to exhibit cancer selectivity even in the same pH medium. There are other factors that may influence this cancer selectivity depending on the mechanisms of action of the peptide. For example, some (but not all) antimicrobial peptides induce oxidative stress in the target cell. Since the distinct metabolism of cancer cells can also induce greater oxidative stress, it is possible that additional stress caused by a peptide cannot be tolerated to the extent it

is in healthy cells.

Tissue selectivity

The strong pH-dependence of cytotoxicity for Dap-rich peptides to PANC-1 cells (Figure 3) indicates that Dap protonation upon medium acidification is coupled with the formation of cationic and toxic peptide species. Here, a phenomenological two-state model was used to describe the observed pH-dependent cytotoxicity of 8Dap. Assuming that the peptide exists in two states, a more cationic, more toxic form and a less cationic, less toxic form, their equilibrium can be expressed as

$$\text{more toxic form} \leftrightarrows \text{less toxic form} + n\text{H}^{+} \quad (2)$$

with a single apparent acid dissociation constant K_a^{app} where

$$(K_a^{app})^n = \frac{[more\ toxic\ form]}{[less\ toxic\ form][H^+]^n} \quad (3)$$

The fraction of the more toxic form F_{mtox} in the total peptide is calculated as

$$F_{mtox} = \frac{1}{10^{n(pH-pK_a^{app})}+1} \quad (4)$$

The fraction of the less toxic form F_{ltox} equals to 1–F_{mtox}. The parameter *n* was semiempirically treated as an adjustable parameter (the Hill constant), which reflects the degree of cooperativity in the pH dependence. We found that $n \sim 1$ gave the best fit for the pH-dependent cytotoxicity of 8Dap (data not shown); therefore, *n* was fixed to unity in the following analysis. Analogous to eq. (1), the cell viability *V* was calculated as a product of viabilities originating from the less toxic form and the more toxic form

$$V = \frac{100}{\left\{1+\left(\frac{C \cdot F_{mtox}}{EC_{50}^{mtox}}\right)^{a}\right\}\left\{1+\left(\frac{C \cdot F_{ltox}}{EC_{50}^{ltox}}\right)^{a}\right\}} \quad (5)$$

where EC_{50}^{mtox} and EC_{50}^{ltox} mean the EC_{50} values of the more toxic and less toxic forms, respectively. The pK_a^{app}, EC_{50}^{mtox}, EC_{50}^{ltox} and *a* values were estimated by globally fitting the observed V values at different pH points (Table 4, Figure 10). As shown in Figure 10, the best fit well reproduced the viability data at each pH, indicating that the two-state model can explain the results well. Although the above phenomenological model oversimplifies the actual 8Dap protonation equilibria involving intermediate species, it provides rough estimates for the EC_{50} values of the more toxic form (~4 μM) and the less toxic form (~100 μM).

The effective pK_a values of Dap-containing peptides may actually be lower than the pK_a of Dap (~6.3). This can be a beneficial effect and actually enhance the selectivity of the peptides. This is because, according to the Gouy-Chapman model, the interface region approaching a negatively charged surface (as in the PANC-1 cells and POPS-containing LUVs) will have lower pH than the bulk.

Mechanisms of cytotoxicity

Overall, the cellular uptake (Figure 5) and cytotoxicity (Figure 3) of the peptides appear to be correlated with their binding affinity to plasma membrane-mimicking anionic lipid bilayers (Figure 7). For example, at acidic pH, 8Dap exhibited higher affinity to anionic membranes via electrostatic interaction, and was efficiently uptaken into the cytosol, leading to cytotoxicity. On the other hand, at neutral pH, 8Dap exhibited lower affinity to the vesicles, poor cellular uptake, and lower cytotoxicity. As indicated by the disappearance of Mito Tracker fluorescence, the internalized peptides could exert cytotoxicity via mitochondrial damage similarly to magainins, as previously reported.[23] It should be noted that the extracellular pH does not influence the intracellular pH, so only the amounts of uptaken peptides determine the mitochondrial damage. To further examine cytotoxic mechanism of Dap-containing peptides, the ability of the peptides to induce endosomal escape of cargo was examined by using a FITC-dextran (Supporting Figure S3). The percentage of cells that exhibited dextran diffusion into the cytosol was 10% or smaller even in the presence of the peptides.

The membrane-bound 8Dap exhibited a flattened CD signal at acidic pH despite its membrane affinity being comparable to that of 0Dap. The lower helicity of the Dap-containing peptide than that of its Lys analog was also reported in a previous study.[24] The protonated Dap amino group can form a hydrogen bond with a carbonyl group of the main chain,[25] resulting in the formation of a stable six-membered ring. This hydrogen bond may stabilize non-helical conformations by perturbing

hydrogen bonds in the main chain.

Interestingly, 8Dap exhibited lower membrane-permeabilizing activities than 0Dap at both physiological and acidic pH values, presumably because the shorter Dap side chain in the hydrophilic surface leads to lower hydrophobicity of the peptide compared to 0Dap. The lower membrane permeabilization activity of 8Dap is consistent with its lower cytotoxicity at physiological pH, while its higher cytotoxicity at acidic pH despite a similar membrane-permeabilizing activity to that at pH 7.4 suggests the presence of cytotoxic mechanisms other than direct peptide–bilayer interactions.

Conclusion

We succeeded in endowing ART properties to the magainin-based peptide 0Dap to enhance its cancer selectivity. Dap incorporation reduced undesired toxicity to normal cells at physiological pH, while maintaining anticancer activity to multidrug-resistant cancer cells at tumor tissue-specific acidic pH. At acidic pH, 8Dap exhibited higher affinity to plasma membrane-mimicking lipid bilayers and was accordingly internalized into cells more effectively than at physiological pH. The affinities depended on the electric charge of Dap. Fluorescence imaging revealed that mitochondria were presumably a major target of the peptides. In summary, 8Dap was internalized into cells in a pH-dependent manner with less plasma membrane damage and depolarized the mitochondria. Incorporation of Dap residues into anticancer peptides will lead to ART peptides that can open a new avenue for treatment of multidrug-resistant cancers with cellular and tissue double selectivities.

Experimental section

Peptide synthesis and purification

The peptides were synthesized by a standard fluoren-9-ylmethoxycarbonyl-based solid phase method as described previously.[14, 26] Alexa488 conjugated peptides (0Dap and 8Dap) were synthesized by mixing a DMF cocktail containing peptide resin, Alexa Fluor488 carboxylic acid (tris salt) (Life Technologies, Carlsbad, CA) and HATU for 48 h. They were deprotected and cleaved from resin with reagent K[26] and purified, and purity was confirmed with reversed-phase high performance liquid chromatography. Purified peptides were identified with matrix-assisted laser desorption ionization mass spectrometery. The concentrations of the peptides were determined based on absorbance at 280 nm.[27]

Cell culture

PANC-1, HEK293 and GM cells were cultured at 37˚C with 5% CO_2 in a humidified incubator. PANC-1 and HEK293 cells were cultured in DMEM medium containing 10 % FBS, 10 units/mL penicillin G, and 10μg/mL streptomycin. GM cells were cultured in CS-C complete medium containing the same additive agents described above. Cells were passaged every 3-4 days.

pH-dependent cytotoxicity

Cells were plated on a 96-well plate and incubated in a culture medium for 24 h at neutral pH. HEPES

and MOPS were added at 10 mM and HCl was used to adjust the pH of the medium in the cytotoxicity experiments and the medium was incubated in a humidified atmosphere over the weekend to achieve CO_2 equilibrium in the atmosphere. After treatment with peptide solutions in the pH-adjusted medium, the cells were incubated for 24 h without CO_2 supply. The change in pH was negligible (≤ 0.1) Cell viability was determined by the Cell Proliferation Reagent WST-1 (Roche, Mannheim, Germany). [28] The medium was gently replaced with 110 μL of fresh pH-adjusted medium containing 10 μL of WST-1 reagent. The pH value of the WST-1-containing culture was adjusted to 7.4 to avoid a weak WST-1 reaction at acidic pH.[29] Several hours (3 h for PANC-1, 2.5 h for HEK293,4 h for GM in pH6.0 and 2 h for GM in pH 6.0) after replacement, the absorbance was measured through a 450−655-nm filter. HEK293 cells were treated only at pH 7.4 because the cells incubated even without the peptides at pH 6.0 did not show enough absorbance in the WST-1 assay.

Peptide uptake in PANC-1 cells

PANC-1 cells (5,000 cells/well) were plated on 96-well optical bottom plates with a coverglass base, allowed to adhere and treated with 0.2 μM Alexa488-conjugated 0Dap or 8Dap in the same manner as for the cytotoxicity assay. In this assay, cells were treated at two pH values, 6.0 or 7.4. After 24 h treatment with Alexa488-conjugated peptides, images of the cells were acquired with a confocal microscope (C1si, Nikon, Tokyo, Japan). A region of interest (ROI) was manually defined for each cell to evaluate uptake of the peptides from the fluorescence intensity of Alexa488 (n = 100).

Mitochondrial potential monitoring

PANC-1 cells (35,000 cells/compartment) were seeded on a 35 mm glass bottom 4-compartment dish (Greiner Bio-One, Frickenhausen, Germany) and incubated for 24 h before being stained and observed. Thirty minutes before the start of peptide treatment, Mito Tracker Red CMXRos (Thermo Fisher Scientific, Bremen, Germany) was added to each compartment at a final concentration of 50 nM. After removal of the culture medium, cells were treated with EC_{50} concentrations of free peptides and 0.2 μM Alexa488-conjugated peptides. The fluorescence of Alexa488 and Mito Tracker were monitored with a confocal microscope for 30 min.

LUVs

LUVs were prepared according to a previous report unless otherwise noted.[14] Briefly, PC and cholesterol were purchased from Sigma (St. Louis, MO) and PS were from Avanti (Alabaster, AL), respectively. A lipid film was hydrated with a buffer (10 mM Tris/150 mM NaCl/1 mM EDTA, pH 7.4) or calcein solution (70 mM calcein, pH7.4) and vortex-mixed to produce multilamellar vesicles. The suspension was incubated at 50 ˚C for 1 h while being vortexed every 15 minutes and then extruded through polycarbonate filters (100 nm pore size filter, 31 times). The lipid concentration was determined in quadruplicate by phosphorus analysis.[30]

Membrane binding

The binding of 0Dap and 8Dap to LUVs was estimated on the basis of Trp fluorescence as mentioned elsewhere[14]. Peptide solutions (4 μM) were titrated with PC/PS/cholesterol or PC/cholesterol liposomes in the Tris buffer (pH 6.0 or pH 7.4) mentioned above at 30 °C while the fluorescence spectra

of the Trp residue were recorded at an excitation wavelength of 280 nm on a Shimadzu RF-5300 spectrofluorometer (Kyoto, Japan). Blank spectra (LUVs) were subtracted and volume correction for dilution (up to 4 %) was performed. Experiments were carried out in duplicate.

CD spectra

CD spectra of 10 μM of 0Dap and 8Dap in the absence and the presence of LUVs (POPC: POPS: chol = 8: 1: 1) in Tris buffer (contains NaF instead of NaCl) were measured on a Jasco J-820 apparatus at 30 ºC using a 1-mm path length quartz cell to minimize the absorbance due to buffer components as reported previously,[14]. We confirmed that the light scattering due to a high concentration of LUVs did not distort the spectrum.[31] Eight scans were averaged for each sample. The blank spectra (LUV suspension or buffer) were subtracted. The % helicity was calculated with ellipticity at 222 nm according to a previous report.[32]

Calcein release assay

The membrane permeabilizing activity was estimated by calcein leakage.[33] The release of calcein from LUVs in Tris buffer (pH 6.0 or 7.4) with or without 1 μM of each peptide was fluorometrically monitored at an excitation wavelength of 490 nm and an emission wavelength of 517 nm. The maximal fluorescence intensity corresponding to 100% leakage was determined by addition of 10% Triton X-100 (20 μL) to the sample (2 mL). The final concentration of lipid in each sample was 5.37 μM. The apparent percent leakage value was calculated according to

$$\%\text{apparent leakage} = 100\,(F - F_0) \,/\, (F_t - F_0) \qquad (5)$$

where F and F_t denote the fluorescence before and after addition of the detergent, respectively and F_0 represents the fluorescence of the intact vesicles.

References

[1] F. Bray, J. Ferlay, I. Soerjomataram, L. Siegel Rebecca, A. Torre Lindsey, A. Jemal, *CA Cancer J. Clin.* **2018**, *68*, 394–424.

[2] D. Lorusso, E. Bria, A. Costantini, M. Di Maio, G. Rosti, A. Mancuso, *Eur. J. Cancer Care (Engl)* **2017**, *26*; R. Oun, Y. E. Moussa, N. J. Wheate, *Dalton Trans.* **2018**, *47*, 6645–6653.

[3] H. P. Varbanov, F. Kuttler, D. Banfi, G. Turcatti, P. J. Dyson, *PLoS One* **2017**, *12*, e0171052/0171051–e0171052/0171016.

[4] Q. He, J. Shi, *Adv. Mater. (Weinheim, Ger.)* **2014**, *26*, 391–411.

[5] M. Zasloff, *Nature (London, U. K.)* **2002**, *415*, 389–395.

[6] D. W. Hoskin, A. Ramamoorthy, *Biochim. Biophys. Acta, Biomembr.* **2008**, *1778*, 357–375.

[7] K. Matsuzaki, *Biochim. Biophys. Acta, Rev. Biomembr.* **1998**, *1376*, 391–400.

[8] D. Vallabhapurapu Subrahmanya, M. Blanco Victor, K. Sulaiman Mahaboob, L. Vallabhapurapu Swarajya, Z. Chu, S. Franco Robert, X. Qi, *Oncotarget* **2015**, *6*, 34375-34388; R. F. A. Zwaal, P. Comfurius, E. M. Bevers, *Cell. Mol. Life Sci.* **2005**, *62*, 971–988.

[9] S. Riedl, D. Zweytick, K. Lohner, *Chem. Phys. Lipids* **2011**, *164*, 766–781.

[10] T. Iwasaki, J. Ishibashi, H. Tanaka, M. Sato, A. Asaoka, D. Taylor, M. Yamakawa, *Peptides (Amsterdam, Neth.)* **2009**, *30*, 660–668.

[11] J. Chiche, M. C. Brahimi-Horn, J. Pouyssegur, *J. Cell. Mol. Med.* **2010**, *14*, 771–794.

[12] R. A. Cardone, V. Casavola, S. J. Reshkin, *Nat. Rev. Cancer* **2005**, *5*, 786–795.

[13] P. Montcourrier, I. Silver, R. Farnoud, I. Bird, H. Rochefort, *Clin. Exp. Metastasis* **1997**, *15*, 382–392.

[14] N. Wakabayashi, Y. Yano, K. Kawano, K. Matsuzaki, *Eur. Biophys. J.* **2017**, *46*, 121–127.

[15] R. A. Cruciani, J. L. Barker, M. Zasloff, H. C. Chen, O. Colamonici, *Proc. Natl. Acad. Sci. U. S. A.* **1991**, *88*, 3792–3796.

[16] E. A. Bell, A. S. L. Tirimanna, *Biochem. J.* **1965**, *97*, 104–111.

[17] G. Roncari, Z. Kurylo-Borowska, L. C. Craig, *Biochemistry* **1966**, *5*, 2153–2159; J. H. Carter, II, R. H. Du Bus, J. R. Dyer, J. C. Floyd, K. C. Rice, P. D. Shaw, *Biochemistry* **1974**, *13*, 1221–1227.

[18] U. J. Meierhenrich, G. M. M. Caro, J. H. Bredehoeft, E. K. Jessberger, W. H. P. Thiemann, *Proc. Natl. Acad. Sci. U. S. A.* **2004**, *101*, 9182–9186.

[19] Y. Lan, B. Langlet-Bertin, V. Abbate, L. S. Vermeer, X. Kong, K. E. Sullivan, C. Leborgne, D. Scherman, R. C. Hider, A. F. Drake, S. S. Bansal, A. Kichler, A. J. Mason, *ChemBioChem* **2010**, *11*, 1266–1272.

[20] N. Raghunand, C. Howison, A. D. Sherry, S. Zhang, R. J. Gillies, *Magn. Reson. Med.* **2003**, *49*, 249–257; O. A. Andreev, A. D. Dupuy, M. Segala, S. Sandugu, D. A. Serra, C. O. Chichester, D. M. Engelman, Y. K. Reshetnyak, *Proc. Natl. Acad. Sci. U. S. A.* **2007**, *104*, 7893–7898.

[21] K. Matsuzaki, K. Sugishita, N. Fujii, K. Miyajima, *Biochemistry* **1995**, *34*, 3423-3429; K. Matsuzaki, *Biochim. Biophys. Acta, Biomembr.* **2009**, *1788*, 1687–1692.

[22] I. Zelezetsky, S. Pacor, U. Pag, N. Papo, Y. Shai, H.-G. Sahl, A. Tossi, *Biochem. J.* **2005**, *390*, 177–188.

[23] H. V. Westerhoff, R. W. Hendler, M. Zasloff, D. Juretic, *Biochim. Biophys. Acta, Bioenerg.* **1989**, *975*, 361–369; L. Cruz-Chamorro, M. A. Puertollano, E. Puertollano, G. Alvarez de Cienfuegos, M. A. de Pablo, *Peptides (N. Y., NY, U. S.)* **2006**, *27*, 1201–1209.

[24] C. Chen, J. Hu, C. Yang, Y. Zhang, F. Wang, Q. Mu, F. Pan, H. Xu, J. R. Lu, *J. Mater. Chem. B* **2016**, *4*, 2359–2368.

[25] P. Batoon, J. Oomens, G. Berden, J. Ren, *J. Phys. Chem. B* **2018**, *122*, 2191–2202.

[26] G. B. Fields, R. L. Noble, *Int. J. Pept. Protein Res.* **1990**, *35*, 161–214.

[27] S. C. Gill, P. H. Von Hippel, *Anal. Biochem.* **1989**, *182*, 319–326.

[28] M. Ishiyama, H. Tominaga, M. Shiga, K. Sasamoto, Y. Ohkura, K. Ueno, *Biol. Pharm. Bull.* **1996**, *19*, 1518–1520.

[29] M. Ishiyama, M. Shiga, K. Sasamoto, M. Mizoguchi, P. G. He, *Chem. Pharm. Bull.* **1993**, *41*, 1118–1122.

[30] G. R. Bartlett, *J. Biol. Chem.* **1959**, *234*, 466–468.

[31] Y. Yano, N. Shimai, K. Matsuzaki, *J. Phys. Chem. B* **2010**, *114*, 1925–1931.

[32] Y.-H. Chen, J. T. Yang, H. M. Martinez, *Biochemistry* **1972**, *11*, 4120–4131.

[33] Y. Miyazaki, M. Aoki, Y. Yano, K. Matsuzaki, *Biochemistry* **2012**, *51*, 10229–10235.

Tables

Table 1 Sequences of MG and MG-based peptides used in this study

Peptide	Sequence[a]	Charge[b]		Difference
		pH 6.0	pH 7.4	
MG	GIGKWLHSAKKFGKAFVGEIMNS	+ 4.5	+ 3.5	1.0
0Dap	GIKKWLHSAKKFGKKFVKKIZNS-NH_2	+ 9.5	+ 8.5	1.0
2Dap	GIKXWLHSAKKFGXKFVKKIZNS-NH_2	+ 8.8	+ 6.7	2.1
4Dap	GIKXWLHSAXKFGXKFVKXIZNS-NH_2	+ 8.1	+ 4.8	3.3
6Dap	GIKXWLHSAXXFGXKFVXXIZNS-NH_2	+ 7.5	+ 3.0	4.5
8Dap	GIXXWLHSAXXFGXXFVXXIZNS-NH_2	+ 6.8	+ 1.1	5.7

[a] Introduced Lys residues are underlined in the 0Dap sequence. X (hatched) and Z represent Dap and Nle residues, respectively.

[b] The charges were estimated based on pH and pK_a values, assuming pK_a values of 6.3, 6.0, and 7.4 for Dap, His, and the N-terminal amine, respectively.

Table 2 Summary of EC_{50} values[a]

	pH 6.0		pH 7.4		
cells	PANC-1	GM	PANC-1	GM	HEK293
0Dap	6.4 ± 0.2	7.6 ± 2.1	9.1 ± 0.3	25.6 ± 4.5	15.7 ± 1.8
2Dap	2.7 ± 0.5	25.9 ± 0.6	14.7 ± 0.6	50.3 ± 0.9	27.2 ± 3.1
4Dap	2.5 ± 0.1	21.1 ± 0.3	35.7 ± 0.7	91.6 ± 5.9	> 100
6Dap	2.5 ± 0.4	19.8 ± 0.3	55.0 ± 1.8	> 100	> 100
8Dap	5.2 ± 0.8	19.2 ± 0.4	61.4 ± 1.7	> 100	> 100

[a]EC_{50} values of each peptide against cancer and normal cells were calculated at pH 6.0 or 7.4.

Each value (mean ± S.D., n = 3) is represented in μM.

Table 3 Helicity of the peptides at each pH[a]

Helicity/%	pH 6.0	pH 7.4
0Dap	63	73
8Dap	17	63

[a]Helicities of 0Dap or 8Dap with liposomes (*L/P* = 100) were calculated based on ellipticities at 222 nm.[32]

Table 4 The best-fit parameters describing 8Dap cytotoxicity by using the two-state model (mean ± S.D., n = 3)

pK_a^{app}	EC_{50}^{mtox} (μM)	EC_{50}^{ltox} (μM)	a
6.1 ± 0.1	3.6 ± 0.8	103 ± 28	2.9 ± 0.3

Figure Legends

Figure 1 Structures of Dap (a) and Nle (b). Nonproteinogenic amino acid Dap and Nle were introduced into an anti-cancer peptide in order to endow pH-responsivity and prevent Met oxidization, respectively.

Figure 2 Drug resistance of PANC-1 cells toward the typical anticancer agent mitomycin C (MMC). PANC-1 cells were incubated with MMC solution for 24 h to confirm the drug-resistance of the cells. The error bars represent S.D. (n = 3). PANC-1 exhibited high viability after MMC treatment both at pH 6.0 and 7.4, confirming the high drug-resistance of PANC-1 cells.

Figure 3 The relationship between medium pH and EC_{50} values for PANC-1 cells. The cytotoxicity assay for each peptide was conducted against PANC-1 cells and the EC_{50} value at each pH was calculated with equation (1). The error bars represent S.D. (n = 3). While Dap introduction did not alter cytotoxicity greatly at weakly acidic pH, it reduced toxicity of the peptides significantly at physiological pH.

Figure 4 The relationship between peptide concentration and cell viability. The viability of each cell type under each condition was compared for 0Dap (a), 2Dap (b), 4Dap (c), 6Dap (d), and 8Dap (e). The error bars represent S.D. (n = 3). While 0Dap showed little pH-dependence, it increased with the Dap number.

Figure 5 Distribution of fluorescence intensity of each cell type treated with the peptides. Fluorescence

intensity for each cell type treated with the labeled peptides was quantified by a manually defined ROI, and the distribution of its fluorescence intensity of the ROI is shown.

Figure 6 Cellular uptake of peptides and changes in mitochondrial membrane potential. a, b, c, d, e and f represent 0Dap/pH 6.0, 0Dap/pH 7.4, 8Dap/pH 6.0, 8Dap/pH 7.4, vehicle/pH 6.0 and vehicle/ pH 7.4, respectively. Red and green images indicate Mito Tracker and Alexa488-labeled peptides, respectively. The concentrations of the unlabeled peptides under each condition for a, b, and c were 6 μM, 9 μM, 5 μM and 60 μM, respectively, and the concentration of the labeled peptides was 0.2 μM. Under conditions with high toxicity, rapid internalization of peptides concomitant with the dissipation of mitochondrial membrane potential (arrows) was observed (a–c). The times after peptide treatments are indicated in the figures.

Figure 7 pH-dependent membrane binding of 0Dap and 8Dap at pH 6.0 (a) and 7.4 (b). The wavelengths at the peaks of fluorescence spectra are plotted as a function of the lipid to peptide molar ratio (*L/P*). While the peptides did not bind to LUV without anionic components, they interacted well with LUV containing 10 % of anionic POPS at both pH values. At pH 7.4, 8Dap showed lower affinity to LUV than 0Dap.

Figure 8 CD spectra of 0Dap and 8Dap at pH 6.0 (a) and 7.4 (b). The CD spectra of 0Dap or 8Dap at pH 6.0 and 7.4 were measured. While the peptides formed random coil structures in solution, they formed helical structures in the presence of LUVs containing 10% anionic POPS. The helicities with LUVs were similar,

except for 8Dap at pH 6.0.

Figure 9 Permeabilization of lipid bilayers induced by peptides. Permeabilization induced by the peptides was evaluated by calcein leakage from plasma membrane-mimicking lipid bilayers (POPC: POPS: chol = 8: 1: 1). The percent leakage values for a detergent, Triton X-100 at L/P = 5.37, are shown. The error bars represent S.D. (n = 2). pH-dependence was not observed for either 0Dap or 8Dap.

Figure 10 Global fitting of the viability of PANC-1 cells in the presence of 8Dap under different pH conditions. Solid curves indicate theoretical curves by eq. (5) with fitting parameters in Table 4. Medium pH values are indicated in the figure.

Table-of-Contents text

By introducing the nonproteinogenic amino acid Dap, a pH-responsive anticancer peptide was developed. It exerted over 10-fold increased toxicity at pH 6.0 specific to cancer tissues compared to that at pH 7.4. This strategy will lead to a new mechanism of cancer tissue targeting to enhance cancer selectivity.

Keywords

pH-responsivity, 2,3-diamino propionic acid, magainin 2

Figures

Figure 1

a.

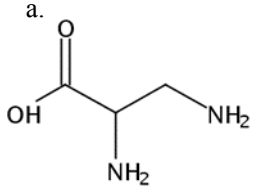

b.

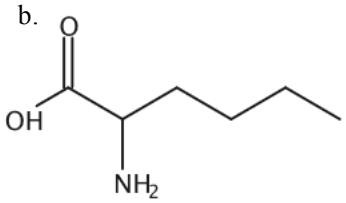

Figure 2

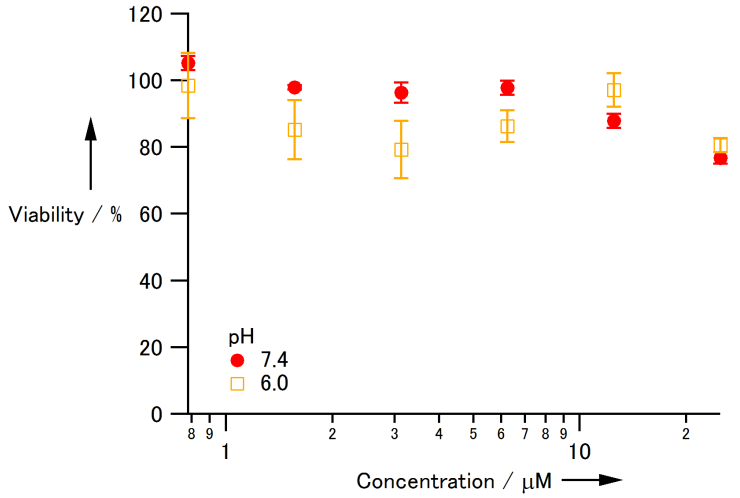
120
100
80
60
40
20
0
Viability / %
pH
7.4
6.0
8 9 1 2 3 4 5 6 7 8 9 10 2
Concentration / μM

Figure 3

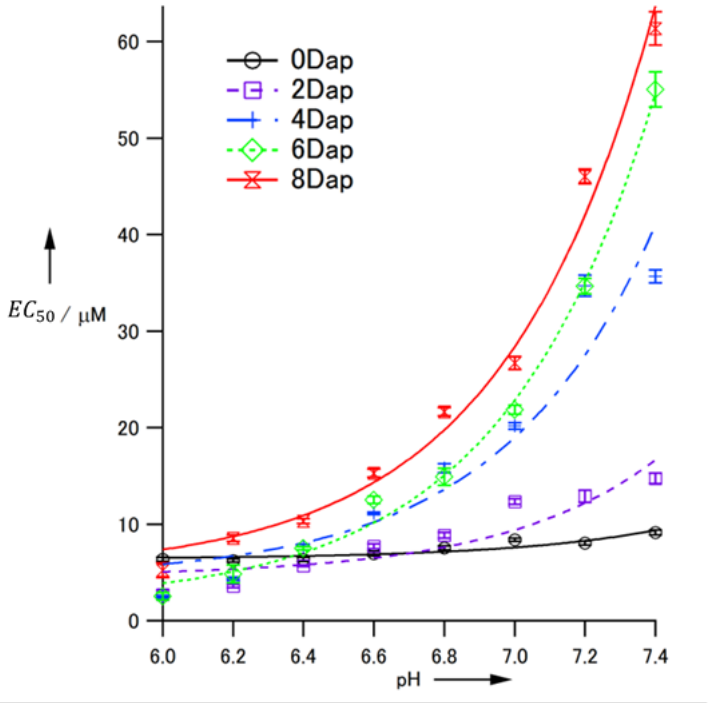
0Dap
2Dap
4Dap
6Dap
8Dap
EC_{50} / μM
60
50
40
30
20
10
0
6.0
6.2
6.4
6.6
6.8
7.0
7.2
7.4
pH

Figure 4

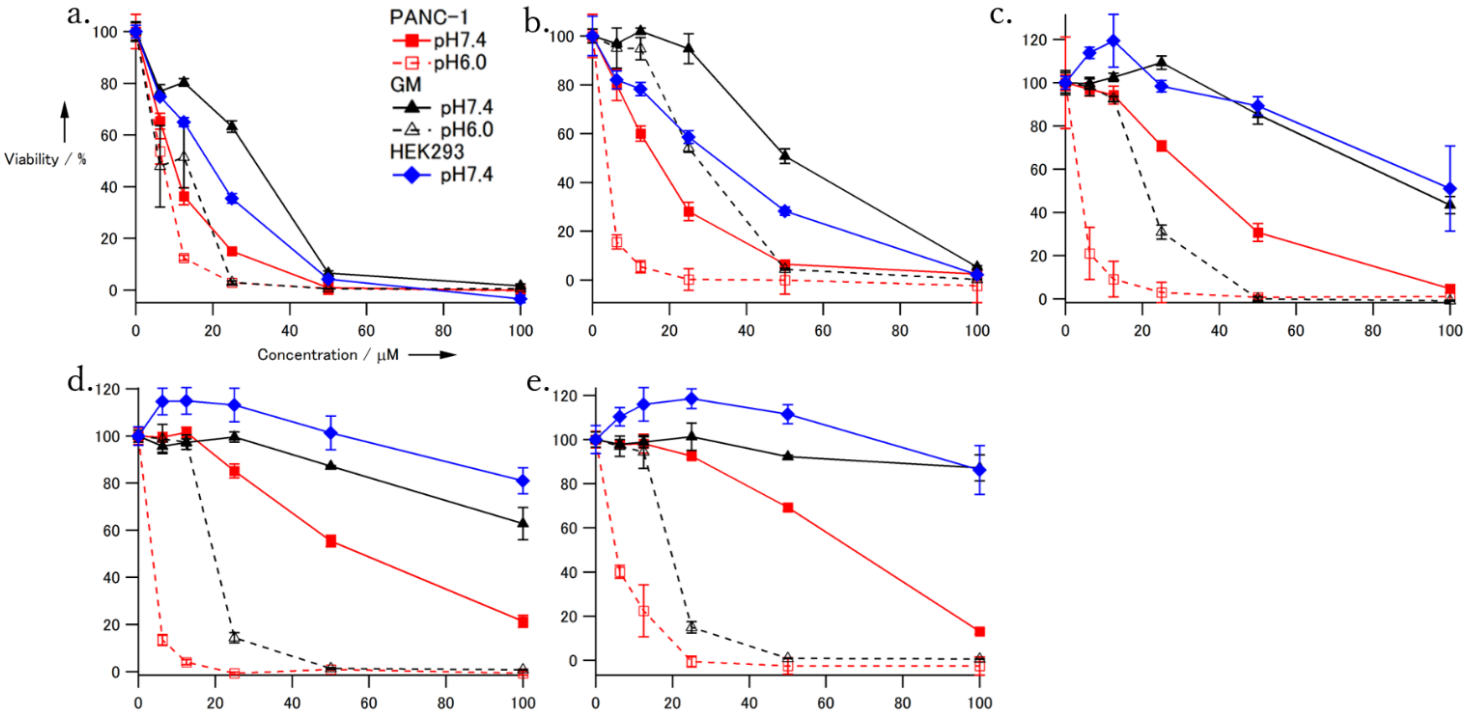
a.
b.
c.
d.
e.
PANC-1
pH7.4
pH6.0
GM
pH7.4
pH6.0
HEK293
pH7.4
Viability / %
Concentration / μM

Figure 5

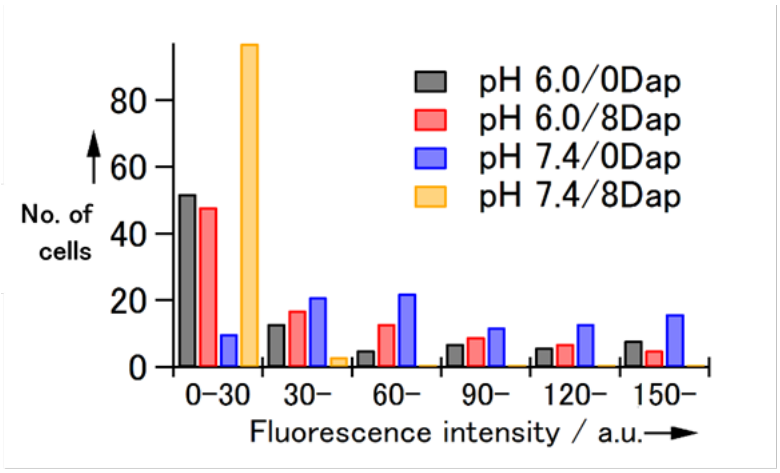
pH 6.0/0Dap
pH 6.0/8Dap
pH 7.4/0Dap
pH 7.4/8Dap
No. of cells
80
60
40
20
0
0–30
30–
60–
90–
120–
150–
Fluorescence intensity / a.u.

Figure 6

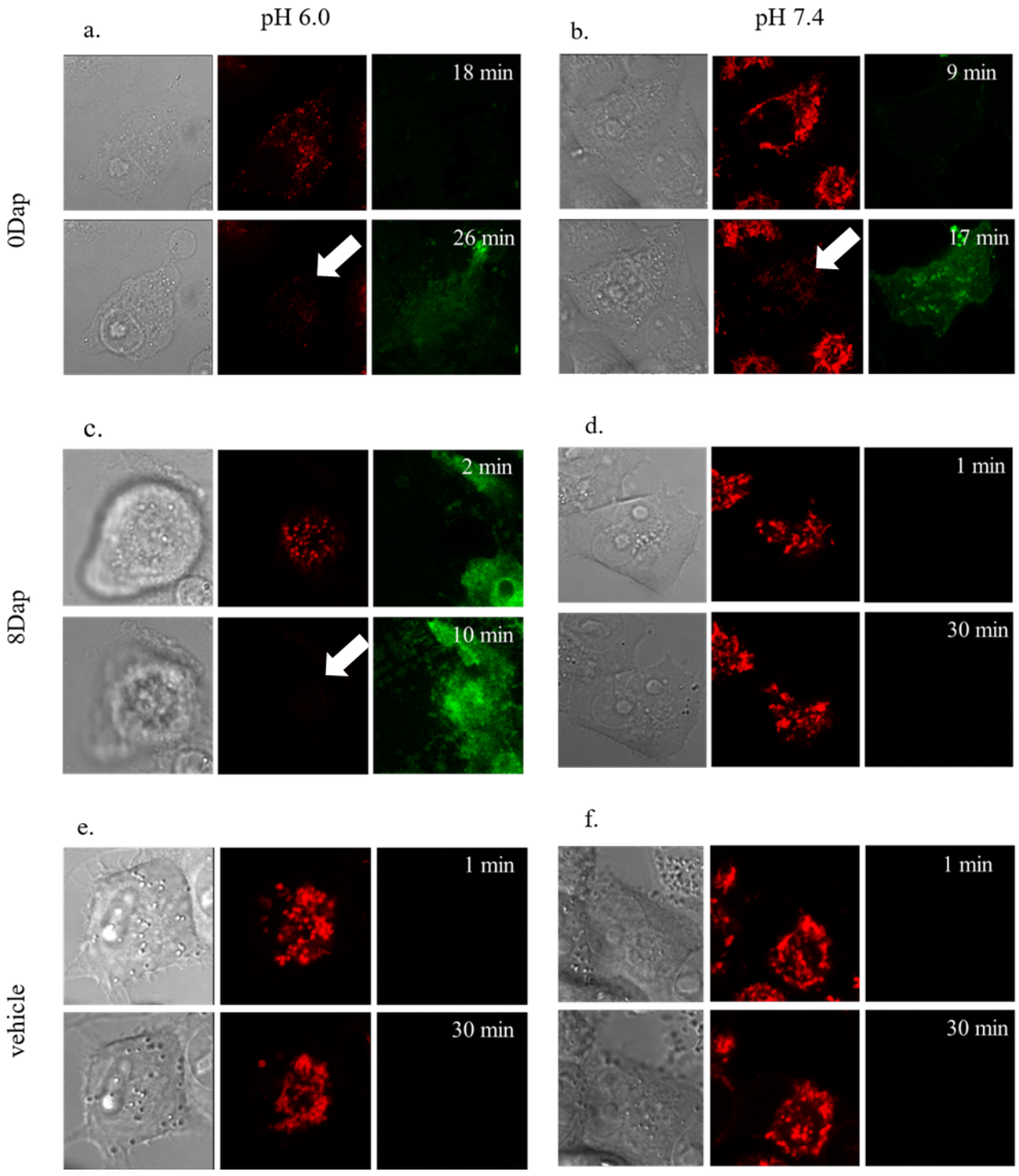
pH 6.0
pH 7.4
a.
b.
c.
d.
e.
f.
0Dap
8Dap
vehicle
18 min
26 min
9 min
17 min
2 min
10 min
1 min
30 min
1 min
30 min
1 min
30 min

Figure 7

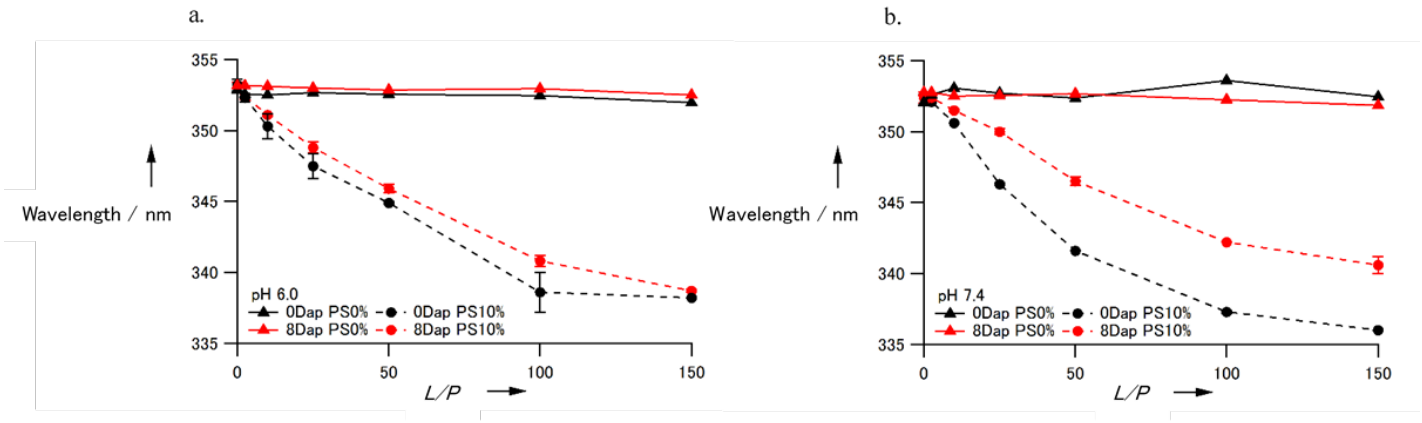
a.
Wavelength / nm
355
350
345
340
335
0
50
100
150
L/P
pH 6.0
0Dap PS0%
0Dap PS10%
8Dap PS0%
8Dap PS10%
b.
Wavelength / nm
355
350
345
340
335
0
50
100
150
L/P
pH 7.4
0Dap PS0%
0Dap PS10%
8Dap PS0%
8Dap PS10%

Figure 8

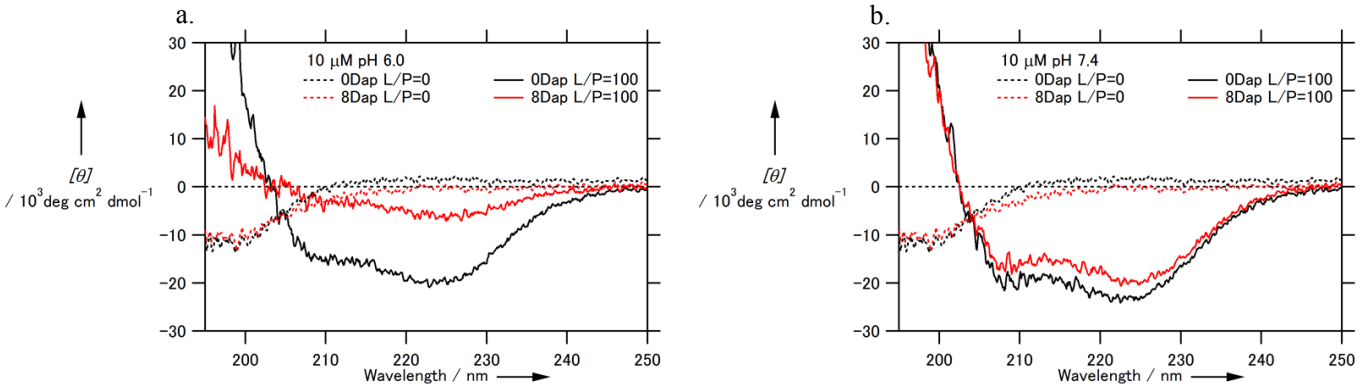
a.
10 μM pH 6.0
0Dap L/P=0
8Dap L/P=0
0Dap L/P=100
8Dap L/P=100
[θ]
/ 10^3 deg cm^2 dmol^-1
Wavelength / nm
b.
10 μM pH 7.4
0Dap L/P=0
8Dap L/P=0
0Dap L/P=100
8Dap L/P=100
[θ]
/ 10^3 deg cm^2 dmol^-1
Wavelength / nm

Figure 9

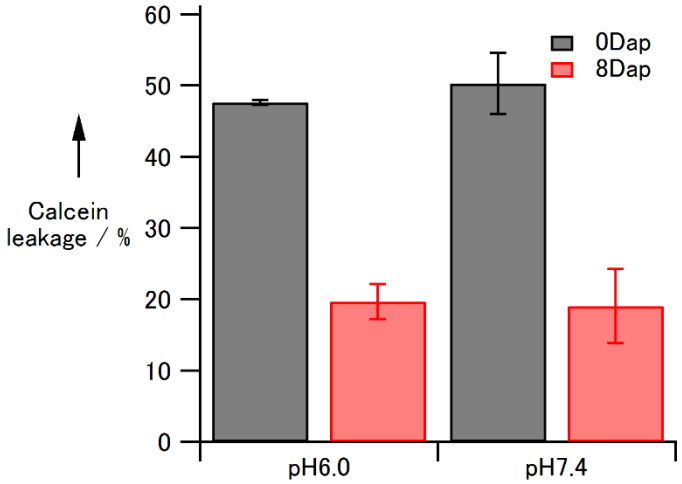

Figure 10

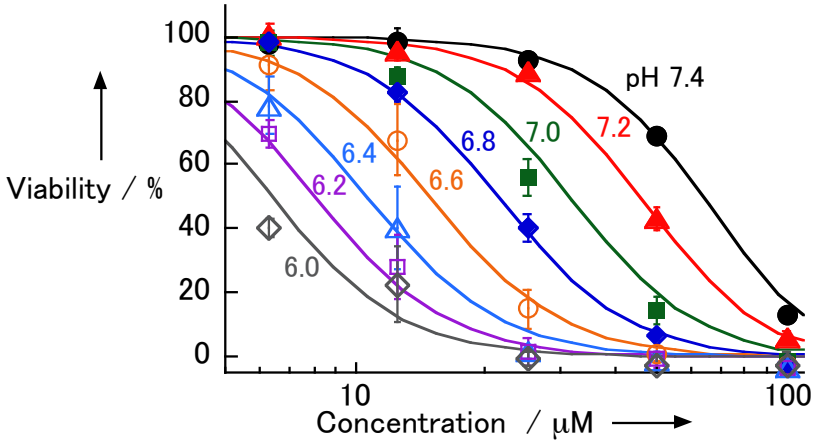
100
80
60
40
20
0
Viability / %
pH 7.4
7.2
7.0
6.8
6.6
6.4
6.2
6.0
10
100
Concentration / μM

Supporting Figures

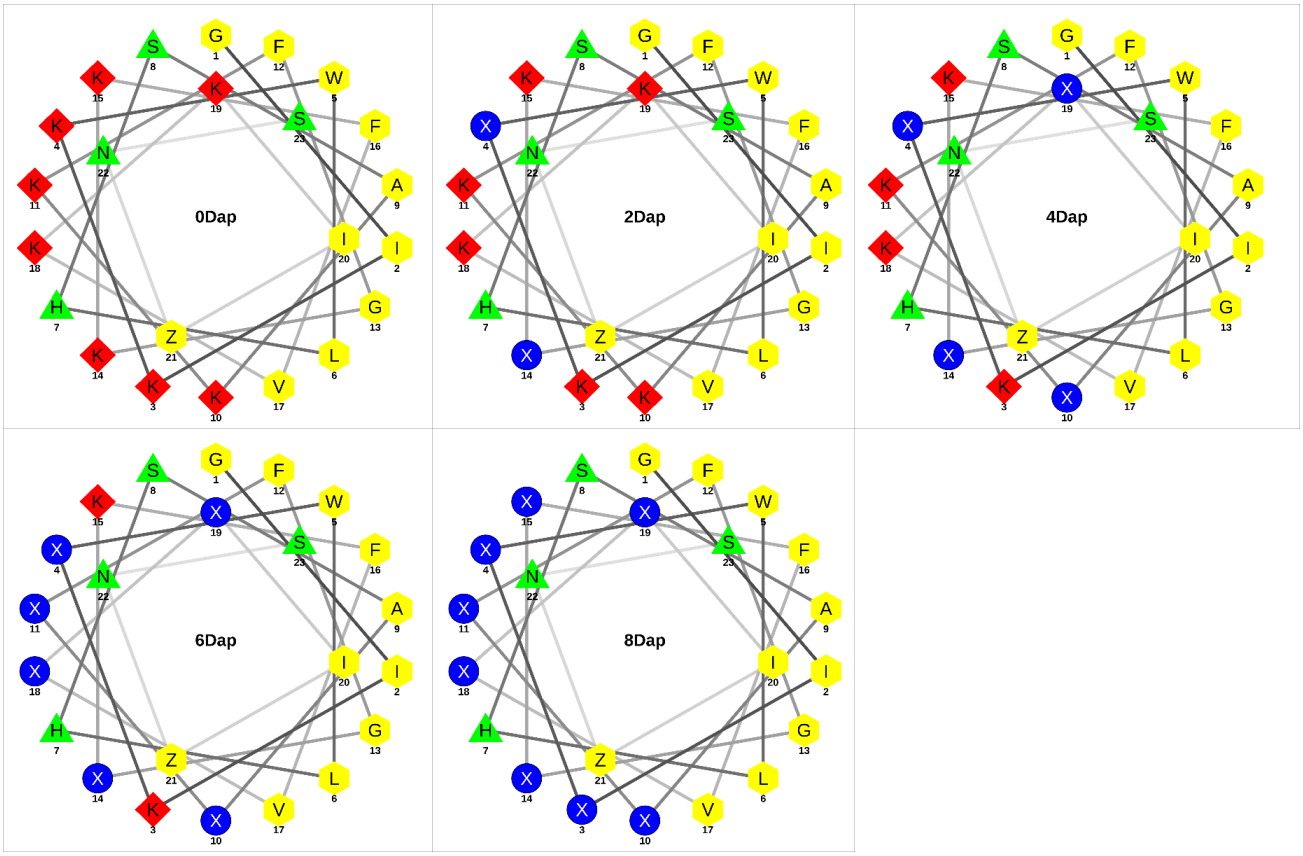

Figure S1. Helical wheel representation of each peptide. The diagrams were generated with a script developed by Alan R. Mól, Wagner Fontes, Mariana S. Castro, Universidade de Brasília – Brazil (http://lbqp.unb.br/NetWheels/). Yellow hexagons, green triangles, red diamonds and blue circles represent nonpolar, uncharged polar, basic polar and Dap residues, respectively.

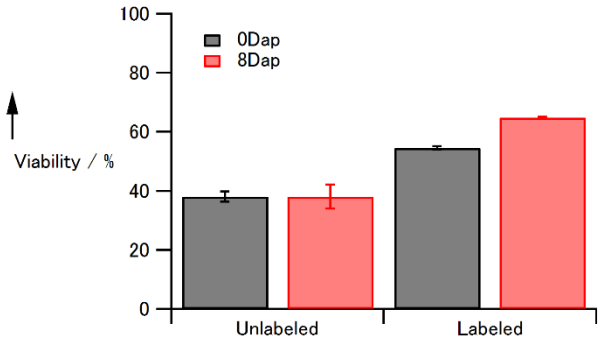

Figure S2 Toxicities of the Alexa488-labeled peptides compared to those of the free-peptides. The peptide concentrations were 6 μM and 5 μM for 0Dap and 8Dap, respectively.

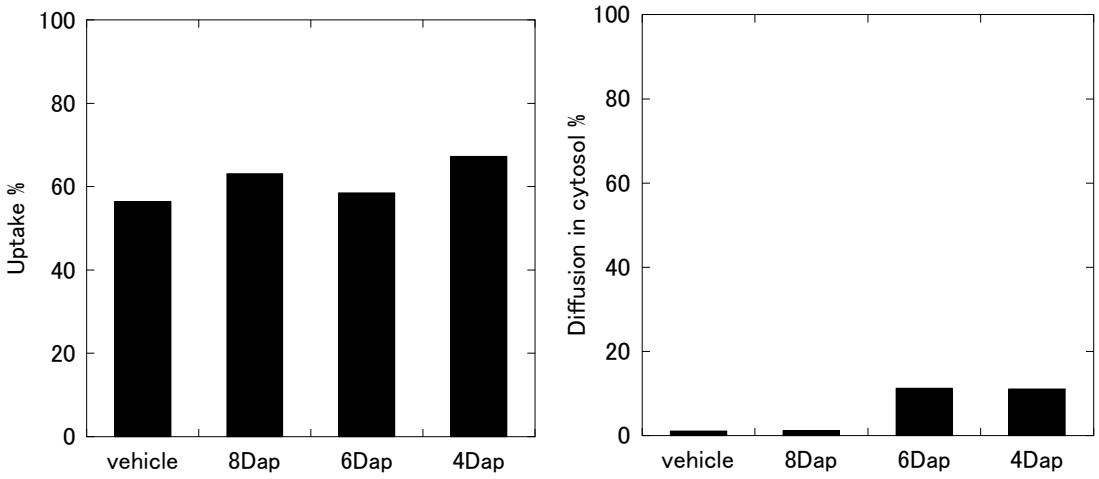

Figure S3 The ability of Dap-containing peptides to induce endosomal escape of cargos. FITC-dextran (70 kDa) was used as a marker. The peptide (10 μM) and FITC-dextran (250 μg mL^{-1}) were co-incubated with PANC-1 cells for 1 h in culture medium. After washout of the dextran and an additional incubation for 3 h, the cells were observed by confocal microscopy. Left and right panels show percentages of cells that exhibited significant vesicular uptake of dextran and dextran diffusion into the cytosol, respectively (n = 186, 358, 258, and 235 for vehicle, 8Dap, 6Dap, and 4Dap, respectively).